

Tree species diversity affects canopy leaf temperatures in a mature temperate forest

Sebastian Leuzinger^{*}, Christian Körner

Institute of Botany, University of Basel, Schönbeinstrasse 6, CH-4056 Basel, Switzerland

Received 29 August 2006; received in revised form 5 May 2007; accepted 9 May 2007

Abstract

Forest canopies play a major role in biosphere–atmosphere interaction. Their actual temperature may deviate substantially from ambient atmospheric conditions as reported by weather stations. While there is a long tradition of false-colour imagery, new digital technologies in combination with IR transmission lenses and autocalibration routines permit unprecedented insight into the actual temperature regimes in canopies. We report canopy leaf temperature distribution over space and time assessed over a 35 m tall mixed deciduous forest in NW Switzerland by means of a construction crane and a high resolution thermal camera. At an air temperature of 25°C, conifers (*Picea abies*, *Pinus sylvestris* and *Larix decidua*) and deciduous broad-leaved trees with exceptionally high transpiration (*Quercus petraea*) or very open, low density canopies (*Prunus avium*) exhibited mean canopy leaf temperatures close to air temperature (0.3–2.7 K above ambient) and the maximum amplitude within a given crown reached 6–9 K. In contrast, broad-leaved deciduous species with dense canopies (*Fagus sylvatica*, *Carpinus betulus* and *Tilia platyphyllos*) were 4.5–5 K warmer than air temperature and showed within canopy temperature amplitudes of 10–12 K. Calculated leaf boundary resistance was clearly lower for conifers (3–24 m s⁻¹) than for broad-leaved trees (33–64 m s⁻¹). The study illustrates that mean leaf temperatures in forest trees are not adequately explained by either stomatal conductance or leaf dimensions, but strongly depend on canopy architecture (leaf area density, branching habits) in combination with leaf traits. Aerodynamic leaf and canopy characteristics lead to strongly enhanced vapour pressure gradients (evaporative forcing) and leaf temperatures vary enormously over short distances, calling for statistical temperature models (frequency distribution) rather than the use of means in any flux calculations. The presence/absence of certain tree taxa plays a key role in forest surface temperature.

© 2007 Elsevier B.V. All rights reserved.

Keywords: Aerodynamics; Leaf energy balance; Infrared thermography; Leaf morphology; Microclimate; Thermal imagery; Plant water relations

1. Introduction

The leaf energy balance and resulting leaf temperature are central themes of biometeorology. Transpiration, sensible heat flux, photosynthesis, respiration and other metabolic activities are driven by leaf temperature. A leaf, on the other hand, also influences its

temperature through stomatal control of transpiration and traits which affect heat exchange (size, shape, angle, pubescence, length of petiole, etc.). On top of these, canopy architecture (height, density, roughness) controls heat and water exchange and thus effective temperatures (Grace, 1977; Jones, 1992). These characteristics may change rapidly (after minutes) in the case of stomatal conductance, or seasonally in the case of leaf angle or leaf position (heliotropism, seasonal shoot growth) or canopy density (seasonal loss of foliage). Long-term changes (many years to centuries) operate through community dynamics, i.e.

^{*} Corresponding author at: Botanisches Institut der Universität Basel Schönbeinstrasse 6 CH-4056 Basel, Switzerland.

Tel.: +41 61 2673511; fax: +41 61 2673500.

E-mail address: Sebastian.Leuzinger@unibas.ch (S. Leuzinger).

the abundance of taxa with certain leaf or canopy characteristics (leaf morphology, size, surface properties, canopy architecture) as well as reflectance and specific leaf water relations. Seasonal phenology also plays a key role. All these features may either increase or decrease canopy temperature, which is then further influenced by dynamic interactions with the atmosphere (Jarvis and McNaughton, 1986). To some extent, trees can engineer their thermal environment and thereby avoid excessive heat or enhance temperatures at otherwise cool conditions. One of the first detailed studies on leaf temperatures across a wide range of taxa and leaf morphologies was undertaken by Ansari and Loomis (1959) using thermocouples. They state that generally, sunlit thin leaves warm ca. 6–10 K above air temperature in still air and ca. 3–5 K with moderate wind speed (5 m/s), a rule of thumb that is still widely valid.

Leaf temperatures are key to many aspects of functional plant ecology. Their significance for plant water relations was acknowledged in the early 20th century (see review by Raschke, 1960), irrigation scheduling by means of canopy temperature surveys has been used in agri- and horticulture since the 1960s (e.g. Fuchs and Tanner, 1966; Jackson et al., 1977; Fuchs, 1990; Jones, 2004). More recently, methods have been developed to accurately estimate stomatal conductance from leaf temperatures (Jones, 1999; Jones et al., 2002; Leinonen et al., 2006). Other applications come from land-surface climate modelling (Dai et al., 2004) to highly topical issues of increasing land surface temperatures caused by global warming (Zaitchik et al., 2006). McElwain et al. (1999) even explain the great turnover of the Triassic–Jurassic megafloora through selection for smaller leaves better adapted to high leaf temperatures.

Large-scale vegetation surveys became possible using satellite infrared images (e.g. Soer, 1980). Various vegetation-related parameters can be estimated from such data, including transpiration (Zhang et al., 2003), plant water stress (Mahey et al., 1991), NDVI (Nemani and Running, 1989) and of course, canopy temperature in their own right (Matsushima and Kondo, 2000).

While surveying vegetation temperatures from aircraft or satellites can cover vast surface areas in a short time, such data are too coarse to account for within-canopy variation and differences between species. Rather than the mean, it is the fine-scale temperature distributions and diurnal variation in temperature which determine heat and gas fluxes. In particular for broad-leaved trees in temperate and tropical forests, canopy temperature may differ substantially among species

Grace (1977). The use of canopy cranes have made it possible to carry out IR-measurements from close enough proximity and with the needed temporal and spatial resolution to provide the species-specific leaf temperatures that are actually experienced under given environmental conditions.

The immediate coupling of leaf temperature with its latent heat loss (Jones and Leinonen, 2003) calls for a description of plant water status parameters, particularly when water supply is highly variable. Temperate forests, however, were found to be the least sensitive low elevation vegetation type to the prolonged 2003 summer drought and heatwave over Europe in terms of canopy temperature and NDVI (Zaitchik et al., 2006). This is in line with concurrent water relations data, showing that at the present study site, it takes over three weeks of continuous drought to significantly reduce daily sap flow peaks (Leuzinger et al., 2005). Therefore, leaf temperature characteristics of deciduous temperate forests are expected to be relatively robust and less dependent on short-term variation in soil moisture than other types of vegetation such as grassland and crops.

The aim of this study was to provide basic data on species specific spatial and temporal canopy temperature distributions of tall temperate zone forest trees. In particular, we compare coniferous and broad-leaved species and ‘open’ versus ‘compact’ tree canopies to explore the significance of forest species composition on canopy heat accumulation. We substantiate our discussion by accounting for leaf morphology and leaf diffusive conductance.

2. Materials and methods

2.1. Site description and studied species

We used a diverse mixed forest stand located 15 km south of Basel, Switzerland (47°28′N, 7°30′E; elevation: 550 m a.s.l., research site of the Swiss Canopy Crane project, Fig. 1). The forest is approximately 100 years old with canopy tree heights between 30 and 38 m. The stand has a stem density of 415 trees ha⁻¹ (diameter ≥ 10 cm), a total basal area of 46 m² ha⁻¹ and a leaf area index of ca. 5 in the experimental area (Pepin and Körner, 2002). It is dominated by *Fagus sylvatica* L. and *Quercus petraea* (Matt.) Liebl., with *Carpinus betulus* L., *Tilia platyphyllos* Scop., *Acer campestre* L. and *Prunus avium* L. present as companion species. In addition, the site has a strong natural presence of conifers (*Abies alba* Mill., *Larix decidua* Mill., *Picea abies* L., *Pinus sylvestris* L.). We henceforth refer to the genus



Fig. 1. Aerial photograph of the Swiss Canopy Crane site in Hofstetten, near Basel, Switzerland. The dominating species are *Fagus sylvatica* and *Quercus petraea*, with *Carpinus betulus*, *Tilia platyphyllos*, *Acer campestre*, *Prunus avium*, *Abies alba*, *Larix decidua*, *Picea abies* and *Pinus sylvestris* as companion species. The canopy height is approximately 30 m with the tallest individuals up to 38 m.

only. A 45-m freestanding tower crane equipped with a 30-m jib and a working gondola provided access to 64 dominant trees in an area of ca. 3000 m² (Fig. 1). Fourteen adult trees have been subjected to a CO₂-treatment since 2001 (Pepin and Körner, 2002). Although these trees showed a mean ca. 15% reduction in whole canopy transpiration (sap flow), this did not lead to measurable canopy warming (>0.3 K) at the scale at which measurements were taken (Leuzinger and Körner, *in press*). Part of the sap flow response resulted from downward adjustment in LAI (in *Fagus*). Therefore, CO₂-treated and non-treated trees were not further distinguished in the current analysis.

The climate is a typical humid temperate zone climate, characterised by mild winters and moderately warm summers. Mean January and July temperatures are 2.1 and 19.1°C. Total annual precipitation at the study site was 950 mm in 2004 and 910 mm in 2005, which is close to the expected long-term average at that site (990 mm), of which two-thirds normally falls during the growing season. The soil is a silty-loamy rendzina that developed on calcareous bedrock. In terms of moisture regime, the two years during which the present study was conducted were average years, and all measurements were carried out at ample soil moisture and clear sky.

2.2. Environmental data and soil moisture

Wind speed, photon flux density, rainfall, air temperature and relative humidity were measured

above the tree canopy using a weather station located at the top of the crane (anemometer AN1, quantum sensor QS and a tipping bucket rain gauge RG1, all from Delta-T, Cambridge, UK). Measurements were performed every 30 s and data were recorded as 10-min means using a data logger (DL3000, Delta-T, Cambridge, UK). Vapour pressure deficit (henceforth referred to as vpd) was calculated from wet and dry bulb, self-made aspiration psychrometer (10-min averages) located at canopy height. Net radiation was measured separately with a net radiometer located ca. 10 m above the canopy (CRN1, Kipp and Zonen, Delft, The Netherlands). Soil water content was measured at ca. 10 cm depth using seven time domain reflectometry probes (ML2x probes, Delta-T, Cambridge, UK) logged hourly in order to provide high time resolution.

2.3. Thermal imaging

We used a state-of-the-art thermal camera (Vario-Cam, Infratec, Dresden, Germany) with a resolution of 240 × 320 pixels, providing 76'800 temperature readings with a 0.1 K resolution. For the type of closed vegetation considered here, a constant emissivity of 98% was assumed (Rubio et al., 1997). For the spatial distribution, we scanned the whole canopy under the crane jib during stable clear sky conditions in midsummer. Canopy regions of similar size and sun exposure were selected for frequency distribution analysis (see Fig. 3). Approximately 5–10 such frames per tree, taken at 5–50 s intervals, were averaged to obtain a temporally and spatially robust pattern of temperature distribution per tree. For the temporal temperature distributions, we took IR-pictures at a frequency of 0.2 Hz (5 s intervals) on two cloud-free days with little wind. We scanned a defined part of the canopy from the counter jib of the crane from 7:30 am to 10 am (true local time) and from 7:30 until 2 pm respectively. Similarly exposed and sized canopy surface polygons were selected to track mean temperature.

2.4. Data processing and statistical analysis

Both for spatial and temporal analyses, thermal images were filtered from what was clearly identified as background and non-leaf temperatures (e.g. branches, forest soil). For temperature series, the mean values were smoothed with an automatic spline function to facilitate graphic representation. For analyses of thermal images, Irbis professional (Infratec, Dresden, Germany) was used. The free software package 'R',

version 2.1.0 ('R' Development Core Team, 2004) was used for all data processing, statistical analyses and graphics.

3. Results

3.1. Water status

The water status of plants is intimately coupled with their foliage temperature. Thus, the interpretation of leaf temperature data requires data on the plants' water supply. For the present study, all leaf temperature measurements were made at ample forest water supply. During the 2004 measurements, mean soil moisture at 10 cm depth was 31 vol. % while during the 2005 measurements, mean soil moisture was 35 vol.%. For the present soil type and climatic conditions, this is a very high soil moisture content (field capacity) and means that trees operated far from shortage of soil moisture and exhibited close to maximum transpiration. From previous studies during the 2003 summer drought, we know that the deciduous species studied here are not very sensitive to even prolonged drought as rated by their stomatal downregulation and sap flow, possible because of deep water storage (no ground water table on these calcareous slopes, Leuzinger et al., 2005). Hence, the leaf temperatures of the studied trees here can be expected to reflect conditions of unrestricted evaporative cooling. Maximal stomatal conductance of the investigated deciduous species ranged from 70 to 340 mmol m⁻²s⁻¹ (Fig. 2, Table 1 and Keel et al., 2007;

Sellin and Kupper, 2004; Handa et al., 2005; Willert et al., 1995).

3.2. Spatial temperature distribution

Canopies were scanned on July 18 2004 from 11:30 to 11:40 true local time at 25.0 °C air temperature and a vpd of 19.7 hPa (Fig. 2). Fig. 3 shows an example of a thermal image with parts of a *Larix* (dark blue, ca. 25 °C), *Quercus* (light blue, ca. 27.5 °C) and *Carpinus* (red, ca. 30 °C) canopy and some selected frames used to compute mean temperatures and temperature ranges shown in Table 1. The false colours also illustrate the wider temperature range seen in the broad-leaved trees opposed to the very narrow range of *Larix*. Except for the very open canopies of *Prunus* (26.7 °C) and the highly transpiring *Quercus* (27.4 °C), all deciduous species showed higher mean leaf temperatures (29.5–29.8 °C) than the coniferous species (25.3–27.0 K, Table 1, Fig. 4). With the exception of *Prunus* (7.3 K) and *Quercus* (8.9 K), the temperature ranges found across a given tree canopy were distinctly narrower in coniferous species (6–8.9 K) than in the broad-leaved deciduous species (10.0–11.8 K). Except for the data of *Pinus*, all frequency distributions were slightly skewed to the upper temperature range. *Larix*, the only deciduous coniferous species, showed by far the lowest canopy temperature, approximately equal to the ambient air temperature.

3.3. Temporal temperature distribution

We measured mean leaf to air temperature difference (ΔT_{L-A}) on June 24 and 28, 2005, two meteorologically similar days (from 07:30 to 10:00 on Day 1, left panels in Fig. 5, and from 07:00 to 14:00 on Day 2, right panels in Fig. 5). Temperature series in Fig. 5 were smoothed with a cubic spline function ('R' Development Core Team, 2004) for the sake of clear visualisation of the rapidly fluctuating signals. Day 1 had a less smooth increase in radiation (some cirrus clouds) which was mirrored by lower ΔT_{L-A} in all species. The three species that were monitored on both days showed very similar patterns of ΔT_{L-A} . With up to 6 K, *Tilia* had consistently the highest ΔT_{L-A} followed by *Fagus* (up to 4.5 K) and *Quercus* (up to 3 K). *Carpinus* was not measured on the second day, but remained ca. 1 K below *Tilia* on the first day. This ranking of ΔT_{L-A} among species confirms approximately the one from the instantaneous ΔT_{L-A} measurements shown in Fig. 4.

As a measure of the short-term temporal variability of the above temperature series $\Delta T_{L-A,t}$, where

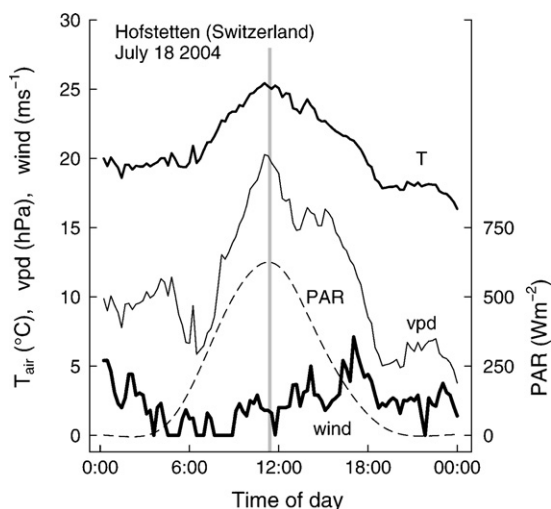


Fig. 2. Vapour pressure deficit (vpd), PAR ($W m^{-2}$), wind ($m s^{-1}$) and air temperature ($^{\circ}C$) during the canopy temperature measurements in 2004 (see Fig. 4). The grey bar indicates the time period when measurements took place.

Table 1

Mean Canopy temperature with number of replicates n , leaf to air temperature difference, temperature range, minimum and maximum, leaf width and the standard error (where applicable) of three coniferous and five deciduous forest trees

Species	n	T_{mean} (°C)	ΔT_{L-A} (°K)	$T\text{-range}$ (°K)	T_{min} (°C)	T_{max} (°C)	Leaf width (mm)	g_s (mmol m ⁻² s ⁻¹)	r_{aw} (s m ⁻¹)
<i>Larix</i>	1	25.3	0.3	6.0	23.4	29.5	0.4±0.04	250 ^a	24.2
<i>Prunus</i>	2	26.7±0.20	1.7	7.3±0.55	24.0±0.25	31.4±0.30	41.2±1.2	237	33.4
<i>Pinus</i>	2	27.0±0.17	2.0	6.3±0.85	23.9±0.70	30.4±0.15	1.3±0.06	120 ^b	2.8
<i>Quercus</i>	12	27.4±0.22	2.4	8.9±0.37	23.3±0.11	32.2±0.36	49.1±1.2	343	49.9
<i>Picea</i>	2	27.8±0.07	2.8	8.9±0.05	24.9±0.10	33.8±0.15	1.2±0.05	125 ^c	12.5
<i>Carpinus</i>	5	29.5±0.21	4.5	10.3±0.24	25.1±0.19	35.6±0.17	36.8±0.8	240	59.9
<i>Fagus</i>	9	29.6±0.34	4.6	10.0±0.37	24.9±0.11	34.9±0.37	45.2±1.0	272	64.9
<i>Tilia</i>	2	29.8±0.88	4.8	11.8±0.30	25.1±0.25	37.0±0.55	72.3±2.0	207	57.8

The two right-most columns indicate the maximum conductances g_s (mmol m⁻² s⁻¹) of 15 bright summer days during 2001–2005 (measurements from the drought year 2003 were excluded) and the calculated leaf boundary layer resistance r_{aw} . Constants used were: $\gamma = 66.5$ Pa K⁻¹ (at 25 °C), $\rho = 1.175$ kg m⁻³ and $s = 189$ Pa K⁻¹. Stomatal conductances are cited from the indicated references where unavailable from the present study site.

^a Handa et al. (2005).

^b Willert et al. (1995).

^c (Sellin and Kupper, 2004).

t annotates time, we calculated the standard errors (S.E.) of the first order differenced time series, i.e. $\Delta^1 \Delta T_{L-A,t} = \Delta T_{L-A,t} - \Delta T_{L-A,t-1}$ (K) where Δ^1 stands for first order differencing characterising the deviation of $\Delta T_{L-A,t}$ from $\Delta T_{L-A,t-1}$. The time step was 5 s, i.e. the frequency 0.2 Hz. Day 1 (left panel of Fig. 5,

only morning hours) showed more short-term variation than Day 2 (right panel of Fig. 5), but there was no significant difference between species within the respective days. On Day 1, S.E. ($\Delta^1 \Delta T_{L-A,t}$) was 3.0×10^{-3} K for *Tilia*, 2.1×10^{-3} K for *Fagus*, $2.8 \times 10^{-3} \pm 0.2 \times 10^{-3}$ K for *Carpinus* and $2.3 \times 10^{-3} \pm 0.1$

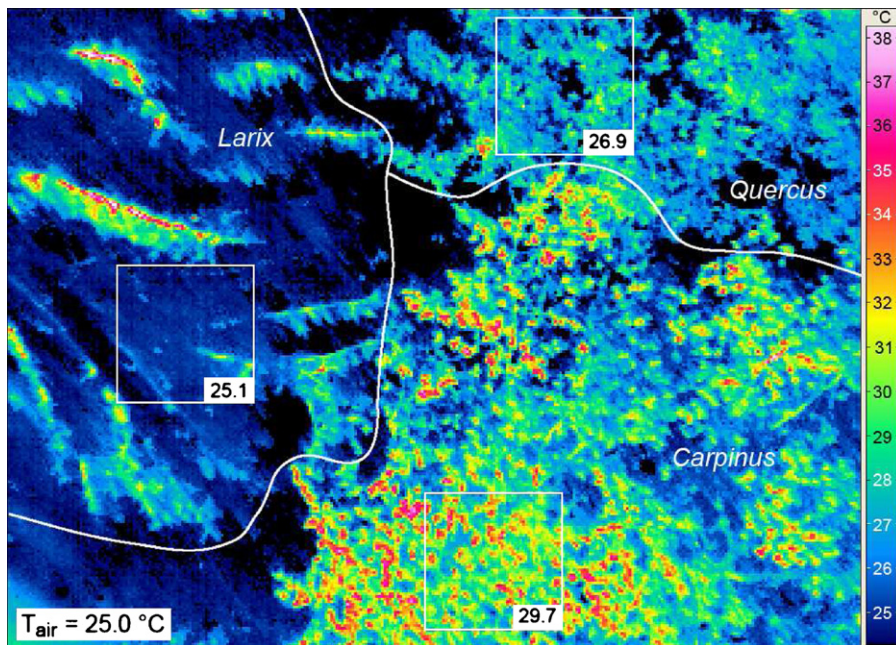


Fig. 3. False colour thermal image taken on August 18 2004, 11:30, showing parts of a *Larix* (left, ca. 25°C), *Quercus* (top right, ca. 27.5°C) and *Carpinus* (right, ca. 30°C) canopy. The squares show some selected frames that have been used to compute mean canopy temperatures shown in Fig. 4. Areas that were clearly showing branch (note for example the linear structures above the left frame which are the monopodial branches of *Larix*) or shaded understorey temperatures (black colour) were either avoided or excluded in the calculations. The *Carpinus* canopy is divided into three major crowns, the center of the tree is lower and not fully sun-exposed.

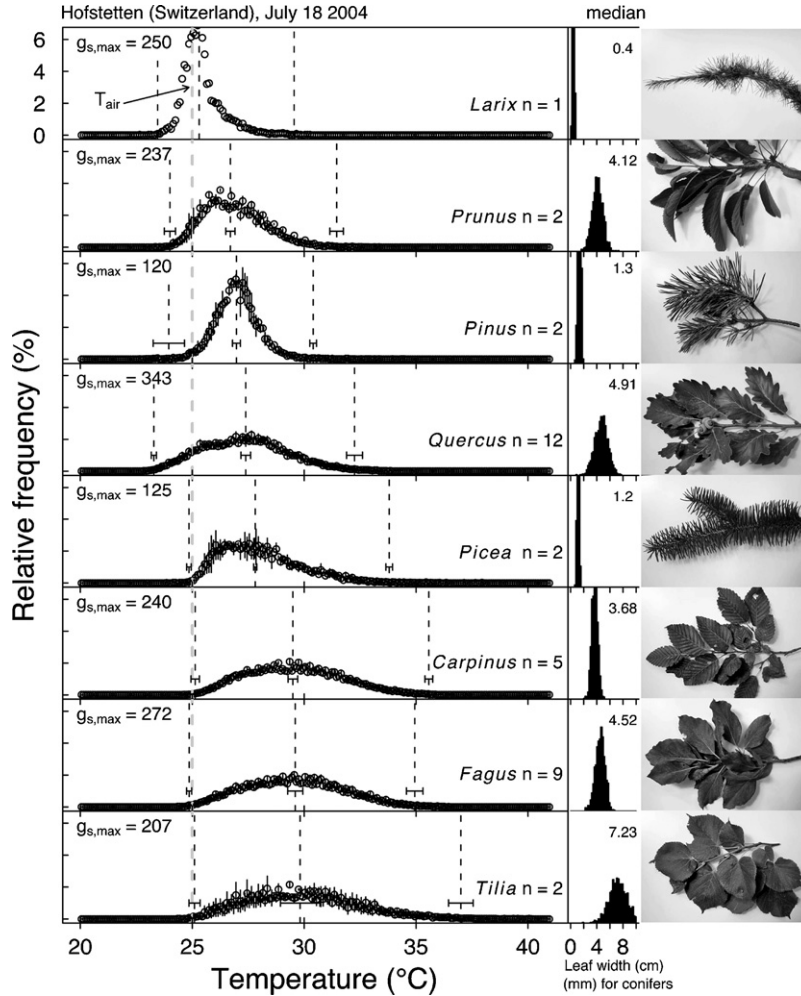


Fig. 4. Leaf temperature distributions (left) and leaf width (right) of the eight different species shown (photos) at an ambient air temperature of 25 °C with standard errors where applicable. Broken vertical lines show minimum, mean and maximum with the according standard errors (horizontal bars). Maximum g_s values are inserted (see Table 1). Note the different scales for coniferous and broad-leaved leaf widths. The mean is indicated in mm in the top right corner.

$\times 10^{-4}$ K for *Quercus*. On Day 2, S.E. ($\Delta^1 \Delta T_{L-A,t}$) was 2.0×10^{-3} K for *Tilia*, $1.6 \times 10^{-3} \pm 0.2 \times 10^{-4}$ K for *Fagus* and $1.4 \times 10^{-3} \pm 0.1 \times 10^{-4}$ K for *Quercus*.

3.4. Estimation of aerodynamic leaf boundary layer resistance

To estimate the leaf boundary layer resistance r_{aW} , we used the leaf energy balance equation of Jones, 1992:

$$\Delta T_{A-L} = \frac{r_{aH}(r_{aW} + r_{lW})\gamma\Phi_n}{\rho_a c_p (\gamma(r_{aW} + r_{lW}) + sr_{aH})} - \frac{r_{aH}\delta e}{\gamma(r_{aW} + r_{lW}) + sr_{aH}}, \quad (1)$$

with air density, ρ_a , heat capacity of dry air, c_p , the psychrometer constant, γ , the net radiation, Φ_n , the slope s of the linearised relationship between the leaf to air temperature difference and the vapour pressure deficit of the air δe . The resistances are defined as follows: the leaf boundary layer resistance to water vapour, r_{aW} , the leaf resistance to water vapour, r_{lW} (the inverse of stomatal conductance), and the leaf boundary layer resistance to heat, r_{aH} . When solved for r_{aW} , the leaf boundary layer resistance to water vapour, we obtain

$$r_{aW} = \frac{\rho_a c_p r_{aH} (\delta e + \Delta T_{A-L} s)}{\gamma (r_{aH} Q_n - \Delta T_{A-L} \rho c_p)} - r_{lW}. \quad (2)$$

Net radiation Φ_n as measured with a net radiometer was 642 W m^{-2} . We varied r_{aH} from 5 to 200 s m^{-1} but

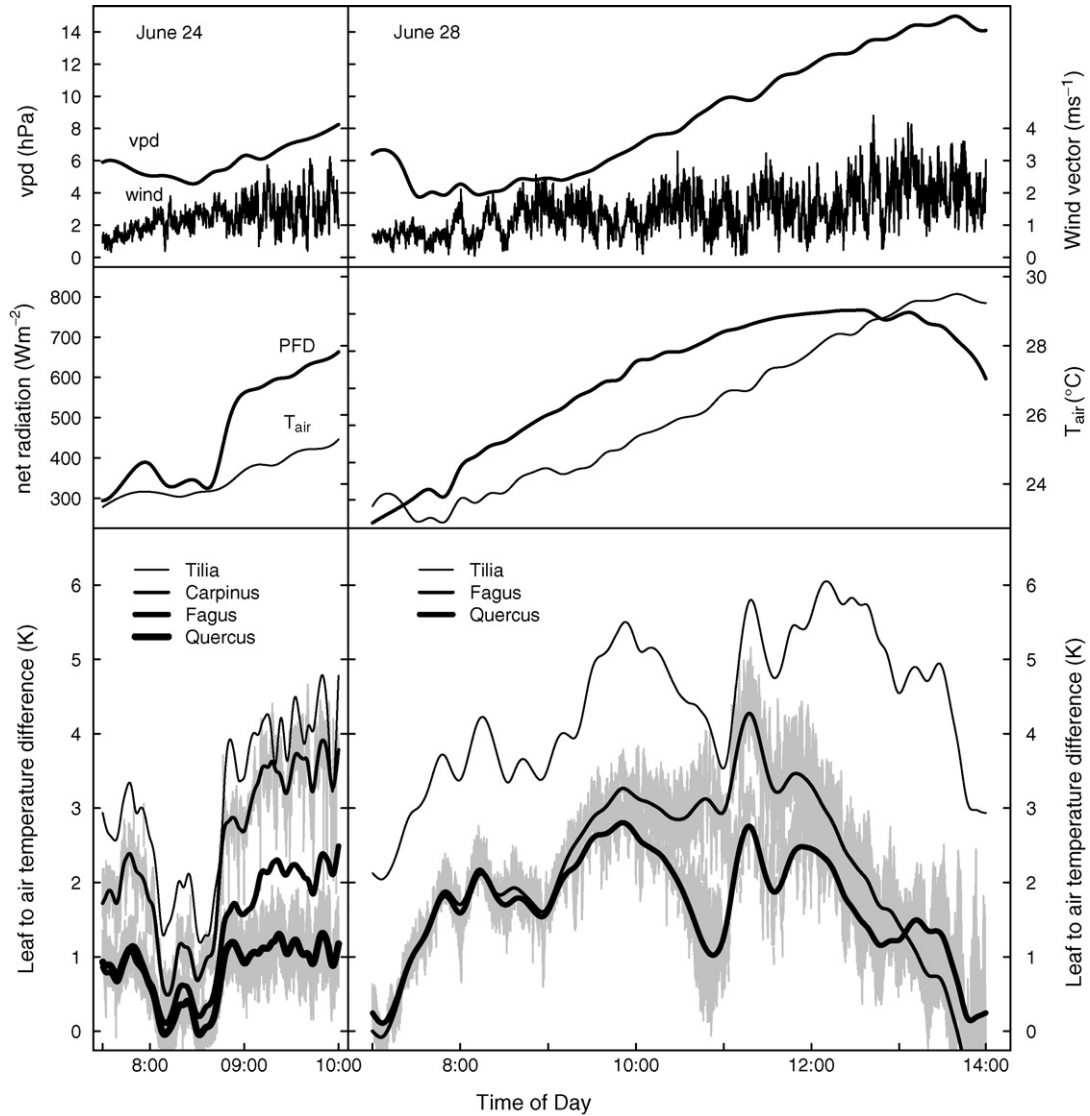


Fig. 5. Leaf to air temperature difference and four environmental parameters at the Swiss Canopy Crane site in Hofstetten during two days in 2005 (Day 1: June 24, left panel; Day 2: June 28, right panel). *Tilia*, *Fagus*, *Carpinus* and *Quercus* with grey vertical bars as standard errors where replication was available (Day 1: *Carpinus*, $n = 2$; *Quercus*, $n = 4$. Day 2: *Fagus*, $n = 3$; *Quercus*, $n = 3$).

since it did not change resistances substantially, it was fixed at 50 s m^{-1} . A constant leaf area index (LAI) of 5 was assumed. It is evident that there are complex feedback effects between leaf temperature and the boundary layer resistances r_{aH} and r_{aW} , but these can be ignored for a rough estimation of r_{aW} with the purpose of combining the information on stomatal conductance with leaf temperature for relative comparisons between species. The resulting leaf boundary layer resistance r_{aW} was higher for the broad-leaved ($33\text{--}65 \text{ s m}^{-1}$) than for the coniferous trees ($3\text{--}24 \text{ s m}^{-1}$, Table 1), confirming the higher level of atmospheric coupling of the latter.

4. Discussion

This study demonstrates that mean canopy temperatures of temperate forest trees deviate substantially from air temperature, but in a highly species-specific manner. On an average summer day, ΔT_{L-A} ranged from nearly 0 K in the aerodynamically well coupled *Larix* to 5 K for *Tilia* with its exceptionally dense canopy structure. Further, canopy temperature ranges became generally wider with mean leaf width, probably because within-leaf temperature ranges also increased with leaf width. Neither mean canopy temperature nor canopy temperature ranges are explained in a straight-forward manner

by leaf width, maximum stomatal conductance or their combination. Rather, it appears that canopy and leaf characteristics (branching, leaf density, angle, thickness, canopy roughness, surface specific radiation energy absorption, instantaneous wind pattern) are causing the final canopy temperature pattern, which can only be determined empirically.

Overall, mean leaf-to-air temperature difference ΔT_{L-A} tracked over time for a subset of species confirmed the temperature patterns found in the analysis of individual pictures (*Tilia* > *Fagus* > *Carpinus* > *Quercus*), except for *Fagus*, which was cooler than *Carpinus* on one day (Fig. 5 left panel). This shows that under constant weather conditions, individual images adequately describe mean canopy temperature distribution, and that long time series may not be necessary. The analysis of the differenced time series as a measure of temporal variability did not show consistent differences between species, although *Tilia* had the highest short-term variability on both days. This may be explained by its more decoupled canopy compared to the other species, resulting in short term changes in radiation having a greater influence and only little buffering by the air temperature (Jarvis and McNaughton, 1986; McNaughton and Jarvis, 1991). The average difference between temperature means of two subsequent images (5 s intervals) was approximately 1×10^{-3} K for all species. This means that average leaf cooling or warming under these fully sunlit conditions occurred at a rate of ca. 0.12 K min^{-1} . The temporal variation in ΔT_{L-A} is partly explained by net radiation (see Fig. 5, left panels), but fluctuations in ΔT_{L-A} of up to 2 K remain entirely unexplained by any of the measured environmental parameters (Fig. 5, right panel). The correlation of ΔT_{L-A} with wind is bad on both days (data not shown), but it is important to note that the wind vector was only measured at one central point within the canopy. The wind patterns actually experienced by the individual tree crowns may have deviated substantially from the shown wind data. The simultaneous decrease in ΔT_{L-A} of *Tilia* and *Quercus* between 10:00 and 11:00 on June 28 is surprising, given the constantly rising net radiation. Likewise, the early decrease in ΔT_{L-A} of *Fagus* and *Quercus* ca. 1 h before the peak of net radiation came unexpected. On the other hand, the fact that several tree individuals simultaneously undergo these temporal temperature patterns suggests that there is no simple shading effect within one specific crown. This can also be confirmed from a visual inspection of the false-colour images. Longer observation periods and multiple wind measurements would be necessary to better understand what causes the temporal ΔT_{L-A} patterns.

We find the variability of the temperature ranges (nearly doubling from *Larix* to *Tilia*) within the different canopies remarkable. The temperature patterns found could be essential in determining the diversity of canopy-dwelling plant and animal communities. A canopy-dwelling spider for example would only be exposed to 23–30 °C in a *Larix* canopy, while if it sat on a *Tilia* canopy, it would be exposed to 25–37 °C. The importance of such canopy temperature differences is potentially greater in the tropics, where high temperatures may be limiting and epiphytes are far more important. In a next step, it is important to see to what extent within-canopy temperatures differ between species and whether they correlate with canopy surface temperatures.

The calculation of the leaf boundary layer resistance r_{aw} combines the cooling effect of transpiration (latent heat loss) and the measured leaf to air temperature difference ΔT_{L-A} . Because we did not estimate the leaf boundary layer resistance to heat (r_{ah}), our calculated r_{aw} values are to be interpreted in relative rather than in absolute terms. They convincingly separate the less coupled broad-leaved (around 50 s m^{-1}) from the more coupled coniferous trees (between 3 and 30 s m^{-1}).

Our results illustrate the importance of tree species composition for the local climate. While the net energy budget for the canopy would perhaps stay the same, a beech-dominated vegetation type would exhibit a surface temperature ca. 5 K higher than for example a larch forest. Such large differences in surface temperature may have consequences for vegetation–atmosphere modelling. For example, Moorcroft (2006) recently pointed out the importance of the inclusion of species diversity in dynamic global vegetation models.

Acknowledgments

We thank Erwin Amstutz and Olivier Bignucolo for crane operations, Roland Vogt for expert advice on thermography and leaf energy balance calculations, the Swiss Federal Office for the Environment (FOEN) and the University of Basel. Financial support came from the Swiss National Science Foundation (NCCR climate, Grant 3100-059769.99 to C. Körner and project P3.2 of J. Fuhrer).

References

- Ansari, A.Q., Loomis, W.E., 1959. Leaf Temperatures. *Am. J. Botany* 46, 713–717.

- Dai, Y.J., Dickinson, R.E., Wang, Y.P., 2004. A two-big-leaf model for canopy temperature, photosynthesis, and stomatal conductance. *J. Climate* 17, 2281–2299.
- Fuchs, M., 1990. Infrared measurement of canopy temperature and detection of plant water-stress. *Theor. Appl. Climatol.* 42, 253–261.
- Fuchs, M., Tanner, C.B., 1966. Infrared Thermometry of Vegetation. *Agron. J.* 58, 597.
- Grace, J., 1977. *Plant response to wind*. Academic Press, London; New York; San Francisco.
- Handa, I.T., Körner, C., Hattenschwiler, S., 2005. A test of the tree-line carbon limitation hypothesis by in situ CO₂ enrichment and defoliation. *Ecology* 86, 1288–1300.
- Jackson, R.D., Reginato, R.J., Idso, S.B., 1977. Wheat canopy temperature—a practical tool for evaluating water requirements. *Water Resources Res.* 13, 651–656.
- Jarvis, P.G., McNaughton, S.J., 1986. Stomatal control of transpiration: scaling up from leaf to region. *Adv. Ecol. Res.* 15, 1–49.
- Jones, H.G., 1992. *Plants and Microclimate*. Cambridge University Press.
- Jones, H.G., 1999. Use of thermography for quantitative studies of spatial and temporal variation of stomatal conductance over leaf surfaces. *Plant Cell Environ.* 22, 1043–1055.
- Jones, H.G., 2004. Irrigation scheduling: advantages and pitfalls of plant-based methods. *J. Exp. Botany* 55, 2427–2436.
- Jones, H.G., Leinonen, I., 2003. Thermal Imaging for the Study of Plant Water Relations. *J. Agric. Meteorol.* 53 (3), 205–217.
- Jones, H.G., Stoll, M., Santos, T., de Sousa, C., Chaves, M.M., Grant, O.M., 2002. Use of infrared thermography for monitoring stomatal closure in the field: application to grapevine. *J. Exp. Botany* 53, 2249–2260.
- Keel, S.G., Pepin, S., Leuzinger, S., Körner, Ch., 2007. Stomatal conductance in mature deciduous forest trees exposed to elevated CO₂. *Trees* 21, 151–159.
- Leinonen, I., Grant, O.M., Tagliavia, C.P.P., Chaves, M.M., Jones, H.G., 2006. Estimating stomatal conductance with thermal imagery. *Plant Cell Environ.* 29, 1508–1518.
- Leuzinger, S., Körner, S., in press. *Global Change Biology*.
- Leuzinger, S., Zotz, G., Asshoff, R., Körner, C., 2005. Responses of deciduous forest trees to severe drought in Central Europe. *Tree Physiol.* 25, 641–650.
- Mahey, R.K., Singh, R., Sidhu, S.S., Narang, R.S., 1991. The use of remote-sensing to assess the effects of water-stress on wheat. *Exp. Agric.* 27, 423–429.
- Matsushima, D., Kondo, J., 2000. Estimating regional distribution of sensible heat flux over vegetation using satellite infrared temperature with viewing angle correction. *J. Meteorol. Soc. Jpn.* 78, 753–763.
- McElwain, J.C., Beerling, D.J., Woodward, F.I., 1999. Fossil plants and global warming at the Triassic–Jurassic boundary. *Science* 285, 1386–1390.
- McNaughton, K.G., Jarvis, P.G., 1991. Effects of spatial scale on stomatal control of transpiration. *Agric. Forest Meteorol.* 54, 279–302.
- Moorcroft, P.R., 2006. How close are we to a predictive science of the biosphere? *Trends Ecol. Evolut.* 21 (7), 400–407.
- Nemani, R.R., Running, S.W., 1989. Estimation of regional surface-resistance to evapotranspiration from NDVI and thermal-IR AVHRR data. *J. Appl. Meteorol.* 28, 276–284.
- Pepin, S., Körner, C., 2002. Web-FACE: a new canopy free-air CO₂ enrichment system for tall trees in mature forests. *Oecologia* 133, 1–9.
- R Development Core Team, (2004). *R: A language and environment for statistical computing*. R Foundation for Statistical Computing, Vienna, Austria.
- Raschke, K., 1960. Heat transfer between the plant and the environment. *Annu. Rev. Plant Physiol. Plant Molec. Biol.* 11, 111–126.
- Rubio, E., Caselles, V., Badenas, C., 1997. Emissivity measurements of several soils and vegetation types in the 8–14 μm wave band: Analysis of two field methods. *Remote Sens. Environ.* 59, 490–521.
- Sellin, A., Kupper, P., 2004. Within-crown variation in leaf conductance of Norway spruce: effects of irradiance, vapour pressure deficit, leaf water status and plant hydraulic constraints. *Ann. Forest Sci.* 61, 419–429.
- Soer, G.J.R., 1980. Estimation of regional evapotranspiration and soil-moisture conditions using remotely sensed crop surface temperature. *Remote Sens. Environ.* 9, 27–45.
- Willert, D.J., Matyssek, R., Herppich, W., 1995. *Experimentelle Pflanzenkologie*. Georg Thieme Verlag, Stuttgart, New York.
- Zaitchik, B.F., Macalady, A.K., Bonneau, L.R., Smith, R.B., 2006. Europe's 2003 heat wave: a satellite view of impacts and land-atmosphere feedbacks. *Int. J. Climatol.* 26, 743–769.
- Zhang, R.H., Sun, X.M., Liu, J.Y., Su, H.B., Tang, X.Z., Zhu, Z.L., 2003. Determination of regional distribution of crop transpiration and soil water use efficiency using quantitative remote sensing data through inversion. *Sci. China Ser. D-Earth Sci.* 46, 10–22.